Using the Artificial Neural Networks for Accurate RF Devices Modeling

LADISLAV POSPÍŠIL JOSEF DOBEŠ
Department of Radio Engineering, Faculty of Electrical Engineering
Czech Technical University in Prague
Technická 2, 16627 Praha 6
Czech Republic

pospisil@jablotron.cz http://www.cvut.cz

Abstract: In the recent PSpice programs, five types of the GaAs FET model have been implemented. However, some of them are too sophisticated and therefore difficult to measure and identify afterwards, especially the realistic model of Parker and Skellern. In the paper, simple enhancements of one of the classical models are proposed first. The resulting modification is usable for reliable modeling of both GaAs FETs and pHEMTs. Moreover, its adjusted capacitance function can effectively serve as a convenient representation of microwave varactors. The accuracy of these models can be strongly enhanced using the artificial neural networks – both using an exclusive neural network without an analytic model and co-operating a corrective neural network with the updated analytic model are discussed. The accuracy of the updated analytic models, the models based on the exclusive neural network, and the models created as a combination of the updated analytic model and the corrective neural network is compared.

Key-Words: Artificial neural network, GaAs FET, optimization, parameters extraction, pHEMT, varactor.

1 Introduction

The Sussman-Fort, Hantgan, and Huang [1] model equations can be considered a good compromise between the complexity and accuracy. However, both static and dynamic parts of the model equations must be modified when using them for possible pHEMT or varactor modeling (i.e., for the devices that are often used in the RF and microwave circuits). All the model modifications defined in the paper have been implemented into the authors' program C.I.A. (Circuit Interactive Analyzer). However, the accuracy of the updated model functions is still of a percentage order. To be more precise, using the artificial neural networks can be the effective and relative simple way because we can utilize the standard MATLAB Neural Network Toolbox. Emphasize that there are two possible ways of using the neural networks. The first consists in approximating the device by an exclusive neural network, the second combines the analytic model with a corrective network.

2 Improvement of the Analytic Model

The diagram of the GaAs FET model is shown in Fig. 1, which is applicable for all five PSpice modeling levels.

2.1 Modifying the Static Part of the GaAs FET Model

The fundamental voltage-controlled current source I_d of the GaAs FET model can be defined for the forward mode (i.e., for $V_\mathrm{d} \geqq 0$) by the updated model functions

$$V_T = V_{T0}\boxed{-\sigma V_\mathrm{d}}, \tag{1a}$$

$$I_\mathrm{d} = \begin{cases} 0 & \text{if } V_\mathrm{g} \leqq V_T, \\ \beta\,(V_\mathrm{g} - V_T)^{n_2}(1 + \lambda V_\mathrm{d})\tanh(\alpha V_\mathrm{d}) & \text{otherwise,} \end{cases} \tag{1b}$$

and by the mirrored equations for the reverse mode ($V_\mathrm{d} < 0$)

$$V_T = V_{T0}\boxed{+\sigma V_\mathrm{d}}, \tag{2a}$$

$$I_\mathrm{d} = \begin{cases} 0 & \text{if } V'_\mathrm{g} \leqq V_T, \\ \beta\,(V'_\mathrm{g} - V_T)^{n_2}(1 - \lambda V_\mathrm{d})\tanh(\alpha V_\mathrm{d}) & \text{otherwise,} \end{cases} \tag{2b}$$

where $V'_\mathrm{g} = V_\mathrm{g} - V_\mathrm{d}$ – see the current and voltages in Fig. 1.

The model parameters V_{T0}, β, n_2, λ and α have already been defined in [1], the parameter σ used in the

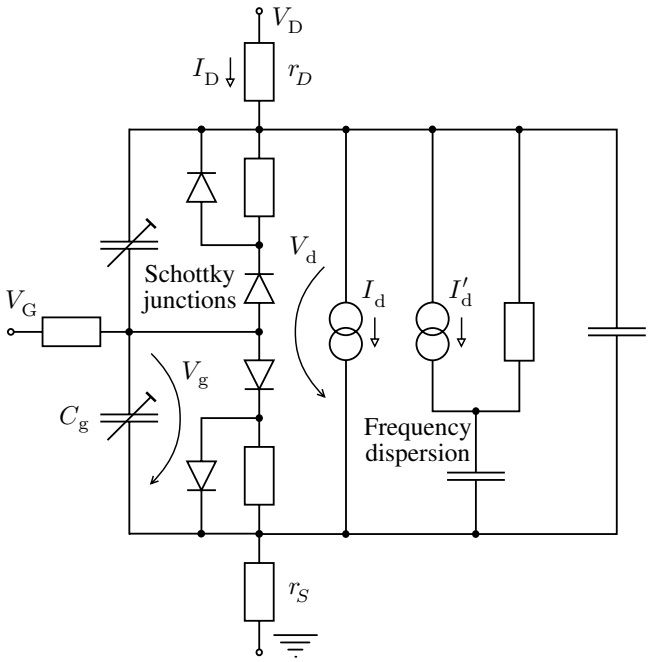

Figure 1: Simplified diagram of the GaAs FET model, which includes the frequency dispersion.

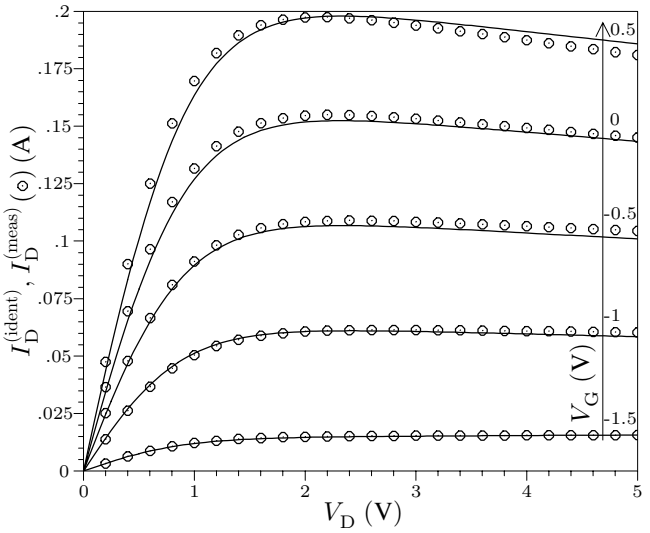

Figure 2: Results of the pHEMT model identification utilizing (1) and (2) ($\mathrm{rms} = 2.38\,\%$ and $\delta_{\max} = 8.24\,\%$). The measured data are taken from [4].

"boxed" parts of (1) and (2) represents the updating of the simpler classical models. Note that the Parker-Skellern realistic model contains similar relations [2] as a part of complicated internal functions – (1a) and (2a) can be considered as their fundamental core.

Although the updated equations (1) and (2) are relatively very simple, they contain an important improvement in comparison with the classical Curtice model [3] (n_2 which characterizes *gate* voltage influence on $I_{\rm d}$ more precisely), and also in comparison with the classical Statz [3] model (σ which characterizes *drain* voltage influence on $I_{\rm d}$ more precisely).

2.2 Using the Modified Model as a pHEMT Representation

The modifications (1a) and (2a) also enable the model to be utilized for the pHEMT modeling – see the results in Fig. 2. The identification process has set the model parameters to $V_{T0} = -1.64\,\mathrm{V}$, $\beta = 0.102\,\mathrm{A\,V^{-2}}$, $n_2 = 0.991$, $\lambda = -0.0288\,\mathrm{V^{-1}}$, $\alpha = 1.16$, $\sigma = 0.00797$, $r_D = 0.3\,\Omega$, and $r_S = 0.2\,\Omega$. As seen in Fig. 2, the representation of pHEMT using (1) and (2) is quite precise ($\mathrm{rms} \approx 2\,\%$ only) and is slightly more accurate than the TriQuint one in [4]. Emphasize that the suggested model is also able to form a negative differential conductance, which is illustrated in Fig. 2. On the other hand, at very high frequencies, the s_{22} parameter does *not* match the DC curves. Therefore, a corrective current source $I'_{\rm d}$ must be added identified by the s parameters measurement. Note that embedding the frequency dispersion can also be performed in another more precise, but more complicated way, see [2].

2.3 Modifying the Dynamic Part of the GaAs FET Model

In general, the GaAs FET gate capacitance is highly nonlinear as shown in Fig. 3. Its definition splits into the three parts [1], similar to those in the Statz and similar models [2, 3]

$$C_{\rm g} = \begin{cases} \epsilon W \arctan\sqrt{\dfrac{\phi_0 - V_T}{V_T - V_{\rm g}}} & \text{if } V_{\rm g} \leqq V_A, \\ \dfrac{V_{\rm g} - V_A}{V_B - V_A}\left[C_{J0}\left(1 - \dfrac{V_B}{\phi_0}\right)^{\boxed{-m}} + \right. & \\ \left. \pi\dfrac{\epsilon W}{2} - \epsilon W \arctan\sqrt{\dfrac{\phi_0 - V_T}{V_T - V_A}}\right] + & \\ \qquad \epsilon W \arctan\sqrt{\dfrac{\phi_0 - V_T}{V_T - V_A}} & \text{if } V_{\rm g} > V_A \\ & \wedge\, V_{\rm g} < V_B, \\ \pi\dfrac{\epsilon W}{2} + C_{J0}\left(1 - \dfrac{V_{\rm g}}{\phi_0}\right)^{\boxed{-m}} & \text{if } V_{\rm g} \geqq V_B, \end{cases} \tag{3}$$

where the transitional region (V_A, V_B) is specified empirically

$$V_A = V_T - 0.15\,\mathrm{V}, \quad V_B = V_T + 0.08\,\mathrm{V}. \tag{4}$$

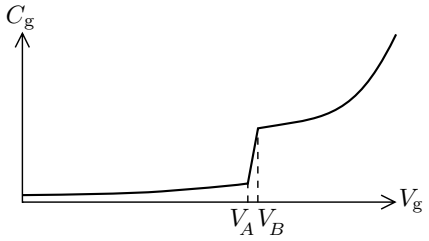

Figure 3: Suggested GaAs FET model function for the varactor representation.

All the model parameters have been defined in [1] with the exception of the "boxed" $-m$. This parameter can be found in the recent PSpice programs only – all the classical models always use the theoretical value $-\frac{1}{2}$ instead of $-m$.

2.4 Using the Modified Model as a Varactor Representation

The microwave varactors are highly nonlinear with observed dependencies similar to those in the GaAs FET gate capacitances. Therefore, the functions in (3) can be utilized after replacing C_g and V_g with the external ones, i.e., with C_G and V_G. Let's emphasize that such "empirical" method is often used in the GaAs FET modeling, especially in [2].

2.4.1 Testing the Varactors of Texas Instruments

Firstly, let's demonstrate this idea by identifying the Texas Instruments EG8132 [5] varactor – see the results in Fig. 4. The identification confirms that the usage of (3) enables more accurate approximation than the 6$^{\text{th}}$ order polynomial that used in [5].

For this varactor, the optimization procedure has given the values of the model parameters $\epsilon W = 0.15711\,\text{pF}$, $C_{J0} = 1.0771\,\text{pF}$, $V_T = -2.7569\,\text{V}$, $\phi_0 = 23.451\,\text{V}$ (!), and $m = 12.827$ (!). Of course, the last two parameters do not have "physical" values, which illustrates the necessity of using the general $-m$-power in (3). From the physical point of view, the varactor is *not* defined for $V_G > V_B$ by the classical junction capacitance function – however, this formula is sufficiently flexible to approximate it.

2.4.2 Testing the Varactor of International Laser Centre

Secondly, the highly nonlinear capacitance model of the optical SACM APD layer structure MO457/4 [6] has been identified. However, obtained results are more inaccurate ($\text{rms} = 6.21\,\%$ and maximum relative deviation $\delta_{\max} = 23.7\,\%$) and therefore a plot of the results is not included at this moment.

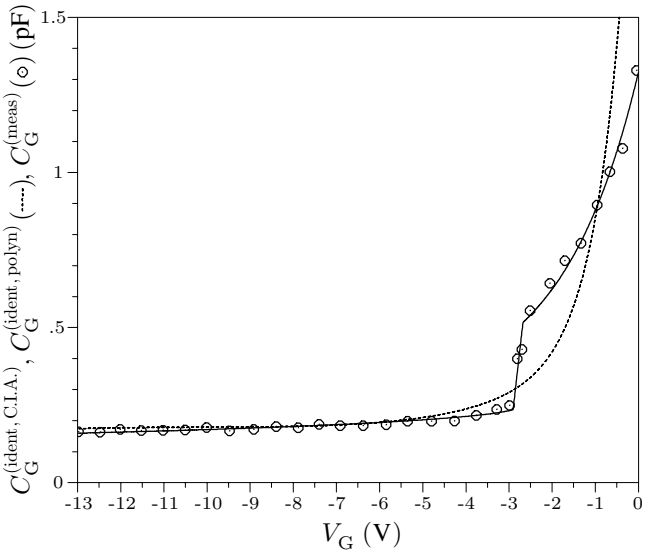

Figure 4: Comparison of the TI EG8132 varactor model identification using (3) with the classical polynomial function ($\text{rms} = 4.52\,\%$ and $\delta_{\max} = 13.7\,\%$ for the model suggested here). The measured data are taken from [5], where the polynomial approximation $a_0 + a_2(V_G - V_a)^{-2} + a_3(V_G - V_a)^{-3} + \cdots + a_6(V_G - V_a)^{-6}$ has also been tested with the inaccurate results shown above (they are drawn by the dashed curve).

3 Applying Artificial Neural Networks

The rms deviations of the analytic models can be of the percentage order – it is clearly illustrated in Sec. 2. To obtain lesser values, the artificial neural networks are often used [7] for modeling the RF devices. A detailed description of the conception of the neural networks can also be found in [7] with the emphasis to modeling the nonlinear RF and microwave devices. There are two main ways for using the artificial neural networks. The first consists in utilizing an exclusive neural network, i.e., without an analytic model, and the second uses a neural network only as a correction tool of the difference between the measured data and the identified analytic model.

3.1 Utilizing the "Exclusive" Artificial Neural Network

A neural network proposed for an approximation of an element without a co-operation with an analytic model can be named as "exclusive". Firstly, the models identified in Sec. 2 have been approximated using the exclusive neural networks to compare their precision with the updated analytic models. Regarding all the artifi-

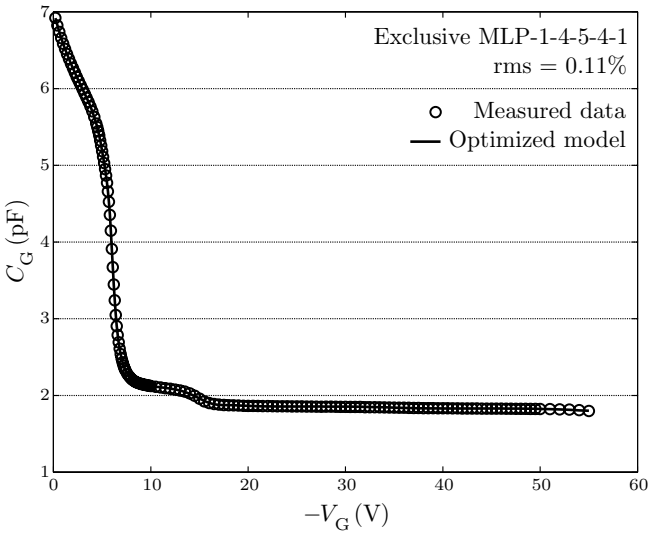

Figure 5: Results of the ILC varactor model identification using the exclusive neural network (maximum relative deviation $\delta_{\max} = 0.4\,\%$ only!).

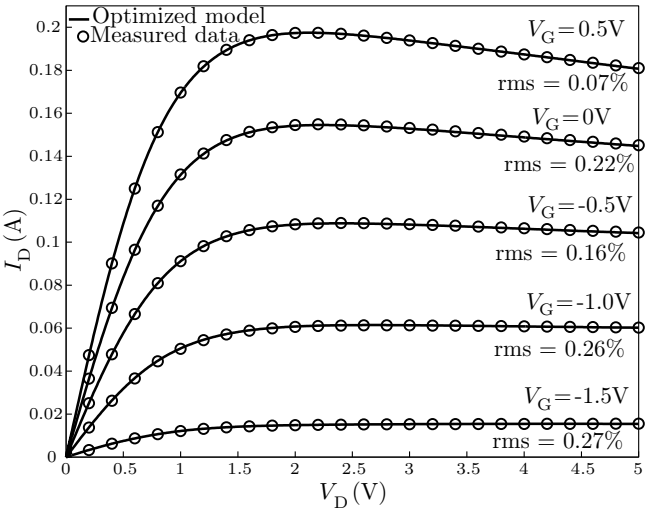

Figure 6: Results of the pHEMT model identification using the exclusive neural network of the MLP-2-5-4-5-1 structure (for all the curves, $\mathrm{rms} = 0.2\,\%$).

cial neural networks, the standard multilayer perceptrons (MLP) structure [7, p. 65] has been used. The number of layers and the number of neurons in that layers have been carefully selected during many numerical tests – the MATLAB Neural Network Toolbox has been used [8] for determining all the weights of the selected neural systems.

3.1.1 Enhancing the Accuracy of the Varactor Model

The ILC varactor model has to be replaced by a neural network because the approximation with the analytic function (3) was not ideal (the values of rms and $\delta_{\max}$ mentioned above). For characterizing the varactor, a simple structure MLP-1-4-5-4-1 (including input/output layers) has been used with the results shown in Fig. 5. Let's emphasize that the accuracy of this neural network is sufficient and hence there is no need to use a corrective neural network with the analytic model (3).

3.1.2 Enhancing the Accuracy of the pHEMT Model

The exclusive artificial neural network has also been used for approximating pHEMT – see the results in Fig. 6 and Table I. Again, a relatively simple structure MLP-2-5-4-5-1 has been selected. As shown in Table I, the accuracy of the exclusive neural network has been approximately ten times better than that for the updated analytical model.

3.2 Utilizing the "Corrective" Artificial Neural Network

Secondly, a neural network can be used as a correction for the updated analytic model. In this case, only the difference between the measured data and previously identified analytic model is approximated using the neural network – such neural network can be named as "corrective". In Fig. 7, the difference between the pHEMT measured data and previously identified analytic model is shown and approximated using the corrective neural network. The resulting accuracy of the updated analytic model with the corrective neural network is shown in Table I. It is clear now that this methodology gives the best precision.

3.3 Limitations of Using the Artificial Neural Networks

The artificial neural networks must be used cautiously. The device must be measured in a large number of points. Otherwise, we could obtain bizarre results as shown for the GaAs FET in Fig. 8 – of course, the number of measured points is here insufficient for the selected structure MLP-2-5-10-7-1.

4 Conclusion

A simple updating of the analytic model has been verified for the approximation of both GaAs FETs and pHEMTs with the precision of a percentage order. An unusual way is suggested for modeling the microwave

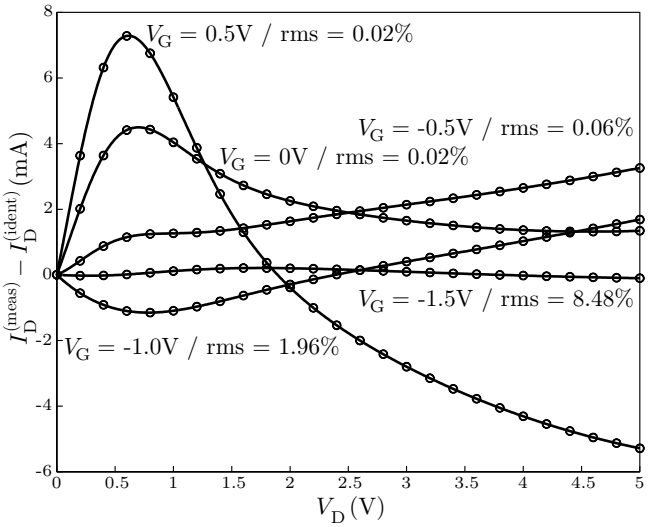

Figure 7: Results of the identification of the *differences* between the measured data and updated analytical model shown in Fig. 2, which is an outcome of the (slightly more complicated) corrective neural network MLP 2-8-10-6-1.

Table 1: Comparison of the accuracy of the updated analytic model (Fig. 2) with the models created using the exclusive (Fig. 6) and corrective (Fig. 7) neural networks, respectively.

V_G (V)	rms (%)		
	Analytic model	Neural network	
		Exclusive	Corrective
0.5	3.23	0.07	0.0006162
0	2.68	0.22	0.0005629
-0.5	2.39	0.16	0.0014
-1	1.85	0.26	0.0362
-1.5	1.23	0.27	0.1043
All curves	2.38	0.2	0.028

varactors using the modified GaAs FET capacitance model function. Finally, using the exclusive and corrective neural networks is tested and compared from the point of view of accuracy. All the model parameters can be easily identified from measured data.

Acknowledgement This paper has been supported by the grant of the European Commission TARGET (Top Amplifier Research Groups in a European Team), by the Grant Agency of the Czech Republic, grant No. 102/05/0277, and by the Czech Technical University Research Project MSM 6840770014.

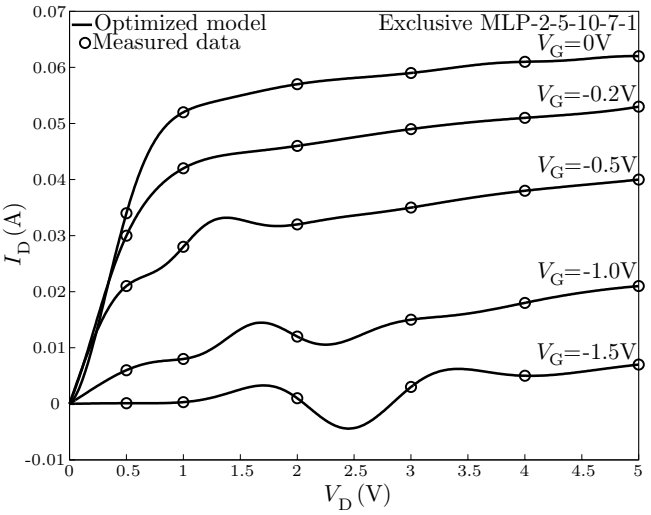

Figure 8: Incorrect results of the DZ 71 [9] GaAs FET model identification caused due to insufficient number of measured points.

References

[1] Sussman-Fort S.E., Hantgan J.C., and Huang F.L. A SPICE model for enhancement- and depletion-mode GaAs FET's. *IEEE Trans. Microwave Theory Tech.*, vol. 34, Nov. 1986, pp. 1115–1119.

[2] Parker A.E. and Skellern D.J. A realistic large-signal MESFET model for SPICE. *IEEE Trans. Microwave Theory Tech.*, vol. 45, Sept. 1997, pp. 1563–1571.

[3] Statz H., Newman P., Smith I.W., Pucel R.A., and Haus H.A. GaAs FET device and circuit simulation in SPICE. *IEEE Trans. Electron Devices*, vol. 34, Feb. 1987, pp. 160–169.

[4] Cao J., Wang X., Lin F., Nakamura H., and Singh R. An empirical pHEMT model and its verification in PCS CDMA system. In *Proc. 29th European Microwave Conference*. Munich, Oct. 1999.

[5] Chang C.R., Steer B.R., Martin S., and Reese E. Computer-aided analysis of free-running microwave oscillators. *IEEE Trans. Microwave Theory Tech.*, vol. 39, Oct. 1991, pp. 1735–1744.

[6] Klasovitý M., Haško D., Tomáška M., and Uherek F. Characterization of Avalanche Photodiode Properties in Frequency Domain. In *Proc. 5th Scientific Conference on Electrical Engineering & Information Technology*. Bratislava, Sep. 2002.

[7] Zhang Q.J. and Gupta K.C. *Neural networks for RF and microwave design*. Artech House, Boston, 2000.

[8] Demuth H. and Beale M. *Neural network toolbox for use with Matlab: User's guide*. The MathWorks, Inc., Natick, 2000.

[9] Jastrzebski A.K. Non-linear MESFET modeling. In *Proc. 17th European Microwave Conference*, 1987.